JOURNAL OF MATERIALS SCIENCE **35** (2000) 2985–2991

Crystallisation of selenium thin films doped with iodine after evaporation

K. D'ALMEIDA, K. NAPO, G. SAFOULA, S. OURO DJOBO, J. C. BERNEDE
Groupe Couches Minces et Matériaux Nouveaux EPSE-2,
rue de la Houssinière-44072 Nantes Cedex 03-France
E-mail: jean-christian.bernede@physique.univ-nantes.fr

Amorphous selenium thin films deposited under vacuum have been doped with iodine either during or after crystallisation. It is shown that when the films are first crystallised at 363 K for 6 h and then submitted to iodine atmosphere at 363 K for 1 h, the structural properties of the films are not modified while their conductivity increases by a factor of 8. Iodine atmosphere induces post crystallisation of amorphous selenium films even at room temperature by increasing the selenium atom mobility at the surface of the films, which induces growth of crystalline spherulites. With annealing, when the heating rate is high (>15 K/min), constraints appear in the films, the density of spherulites increases and the films are inhomogeneous. When the heating rate is small and constant (1 K/min) the interaction between iodine and selenium takes place all over the sample and there is only a small density of small spherulites, while the crystallisation of the whole sample is more homogeneous. XPS and microprobe analysis have shown that the iodine is equally repartitioned in the selenium film. Moreover there is a mixture of neutral iodine and I_3^- as shown by XPS and Raman studies. The high crystalline quality of the films can explain the high conductivity ($>10^{-3}\ \Omega^{-1}\ cm^{-1}$) of these selenium doped films

1. Introduction

Selenium thin films are very easy to obtain by physical vapour deposition and it should be interesting to use it for cheap large-scale device productions such as photovoltaic cells. It has been shown early [1–5] that the morphological evolution of crystallisation in selenium films, in response to thermal treatments, is quite complicated. In particular cylindrites and filamentary crystals form. Often filamentary crystals stem from the more irregular regions of the cylindrites and then grow through the film. These complex structures result in poor electrical performance. An attempt to improve the crystalline properties of selenium thin films has been recently described [6]. Promising results have been obtained by using a thin tellurium under layer. However the samples were quite thin (300 nm) for photovoltaic applications [6]. In earlier papers [7–9] we have shown that when selenium thin films doped with iodine are obtained by evaporation of iodine doped selenium powder there is an increase of three orders of magnitude of the conductivity. This optimum result is obtained by using as starting material a 5000 ppm iodine doped selenium powder. However the maximum value of the conductivity was $1.5.10^{-5}\ \Omega^{-1}$ cm.

We cannot overshoot this result, since, for higher doping concentration, the layers have a large density of pinholes and become inhomogeneous [9]. In this paper we have studied the influence of iodine atmosphere (post iodine doping) on the crystallisation of selenium films. The structural and morphological properties appear to be improved when amorphous films are annealed under iodine pressure.

2. Experimental details

In the case of xerographic [10–12] or rectifying devices [13–15] selenium films were systematically deposited on unpolished substrates in order to prevent any peeling off effect. Therefore, the substrates used in this work were unpolished glass substrates, the averaged roughness being 0.5 μm. The films were thermally evaporated under vacuum (base pressure 10^{-4} Pa) from pure selenium pellets supplied by Aldrich (purity: 99.999%). The substrates were chemically cleaned and then outgassed *in situ* by heating at 400 K for 1 h prior to the deposition of the films. The substrate temperature was controlled by a regulation assembly and monitored using the copper-constantan thermocouple. The selenium evaporation rate ($\cong$600 nm $\cdot$ min^{-1}) and the film thickness (2–10 μm) were measured *in situ* by the vibrating quartz method. The thickness was controlled by a stylus. Two post-doping methods were used. In the first, amorphous selenium films were crystallised by annealing under vacuum at 360 K for 24 h before iodine doping. In the second method, the starting films used were amorphous. Therefore in the first method we dope polycrystalline layers while in the second method we dope and crystallise simultaneously the films. The doping

conditions themselves were the same for the both methods. Selenium films were introduced in a Pyrex tube with a small amount of iodine (some mg). Then the tube was sealed under vacuum. Finally the tube was annealed at a temperature T_a (330 K < T_a < 360 K) for 6 h to 74 h. For comparison, some amorphous films have been crystallised in the same annealing condition but without iodine. Some doping experiments have been carried out at room temperature. Here the glass tube was only stopped up with a cork.

The structural properties of the films were studied by XRD diffraction, by using an analytical X-ray system-type DIFFRACT AT V3.1 Siemens Instrument which uses a graphic program EVA. The X-ray diffractometer uses the monochromatic CuK_α radiation.

X-ray photoelectron spectroscopy (carried out at Nantes with a Leybold spectrometer-University of Nantes C.N.R.S.) was carried out in a commercial photoelectron spectrometer equipped with a twin anode X-ray gun (MgK_α and AlK_α lines at 1253.6 eV and 1486.6 eV respectively). High resolution scans with a good signal to noise ratio were obtained with the magnesium source operating at 10 KV and 10 mA in the selected energy windows. The energy resolution was 1 eV at a pass energy of 50 eV. The quantitative studies were based in the determination of the Se3d, $I3d_{5/2}$, O1s and C1s peak areas with respectively 0.57, 6.4, 0.61 and 0.2 as sensitivity factors (the sensitivy factors of the spectrometer are given by the manufacturer). The glass substrates were grounded with silver paste to avoid charge effect. The efficiency of doping in depth have been checked by recording successive XPS spectra obtained after argon etching for short periods.

As estimated from standard selenium thin films, the rate of sample erosion was approximately 10 nm min^{-1}. Sputtering was performed at pressures of less than 5 10^{-4} Pa a 10 mA emission current and a 5 kV beam energy using an ion gun. Before sputtering the pressure was better than 5×10^{-7} Pa.

Observation of the surface topography of the films was performed using a field-effect scanning electron microscope (JE0L 6400F). Electronic microanalyses using an electron microprobe equipped with a detector were performed in order to control the homogeneity of the distribution of iodine in the films.

For electrical measurements planar samples with a gap electrodes of 1 mm have been used. Metal electrodes were evaporated after doping of the films. Chromium is a good ohmic contact for selenium layers as shown Fig. 1.

The dc resistivity was measured by conventional methods with a Keithley 617 electrometer. During measurements, the currents generated by the electrometer were between 1 nA and 1 pA. Electrical measurements were carried out in the dark at temperatures between 300 K to 520 K.

3. Experimental results

3.1. X-ray diffraction experiments

XRD spectra obtained for different films of the same thickness (5 μm) are reported in Fig. 2.

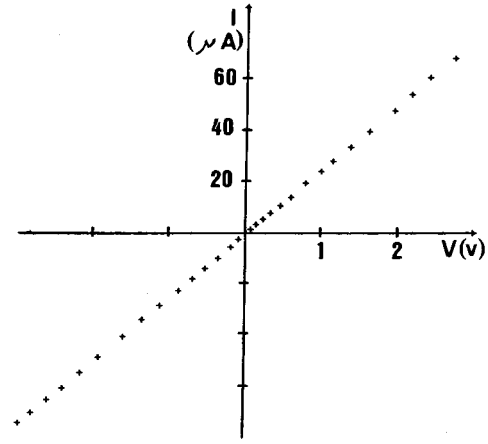

Figure 1 *I-V* characteristics of Cr/Se/Cr structure.

It can be seen that after annealing all the films are crystallised in the trigonal structure of the grey selenium. The peak intensity is small while the full width at half maximum (FWHM) of the diffraction peak is quite broad which means that the films are badly crystallised with very small crystallites.

When the selenium is crystallised before doping (Fig. 2a) its structure is not modified by post doping (Fig. 2b). When an amorphous selenium films is doped at room temperature by iodine there is spontaneous interaction between the selenium film and the iodine gas which induces at least partial crystallisation of the sample (Fig. 2c)

The XRD of a film doped with iodine at 363 K (Fig. 2d) is nearly similar to that of the room temperature doped sample:

A very different result is obtained when the annealing condition is carefully controlled. A progress temperature increasing at a constant rate of 1 K/min achieves the annealing temperature. For the same annealing temperature as in Fig. 2d, the spectrum obtained is that of Fig. 2e: the intensity of the peak is far higher while the FWHM is smaller. In that case the FWHM measured is nearly the same than that obtained with a reference powder which means that the grains are quite large ($\geq$200 nm [16]).

3.2. SEM and microprobe study

Before annealing the films are amorphous and their surfaces are smooth.

After annealing at 363 K for 6 h without iodine, the surface of the films becomes rough. Large grains separated by broad grain boundaries are visible (Fig. 3). It can be seen in Fig. 4 that after an annealing of the films under iodine atmosphere at 360 K for 1 h there is not any modification of the texture of the films and no iodine is detected by microprobe analysis.

After iodine doping at room temperature an amorphous selenium film contains some large spherulites (Fig. 5). Such features are well known to be present in crystallised selenium films, so, it seems that iodine is able to nucleate selenium and to promote the appearance of spherulites.

When annealed at 363 K for 6 h in iodine atmosphere it appears that there is some coalescence effect between

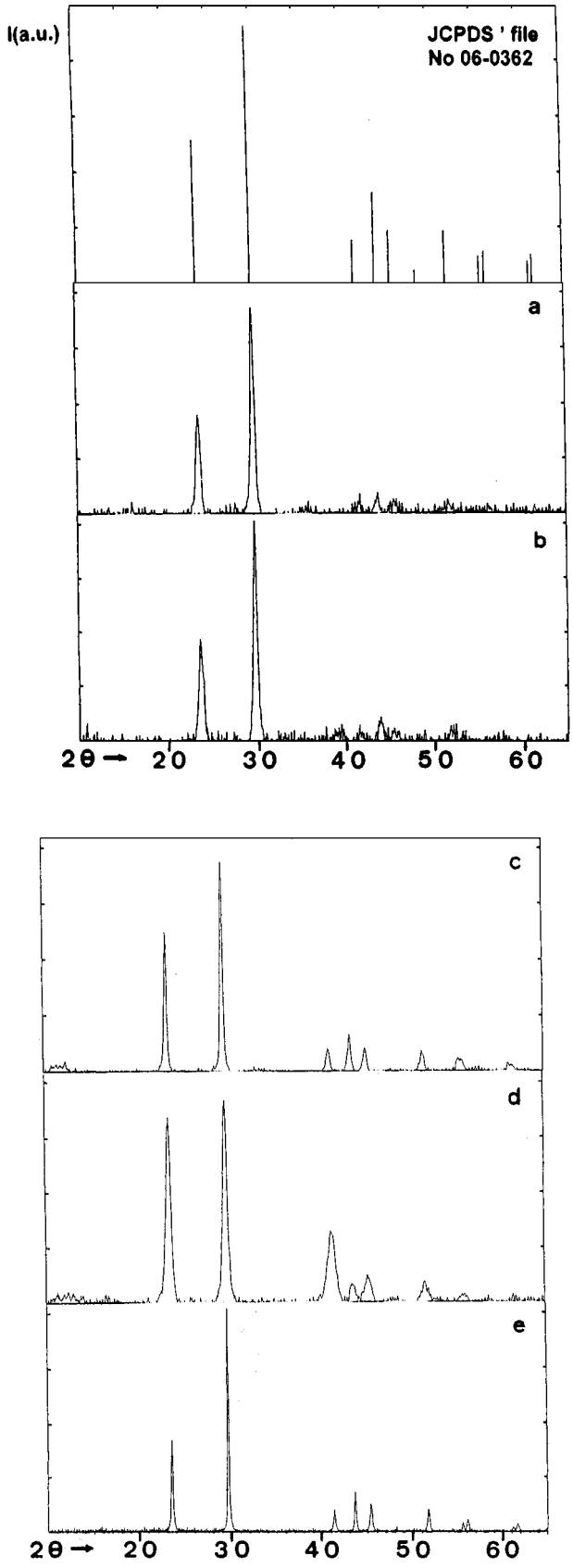

Figure 2 XRD diagrams of selenium films (film thickness: 5 μm), (a) pure selenium film crystallyzed by annealing 6 h at 363 K, (b) selenim film crystallyzed by annealing 6 h at 363 K and post doped by iodine 1 h at 363 K, (c) selenim film doped by iodine at room temperature ($T = 300$ K), (d) selenim film doped by iodine at $T = 363$ K for 6 h, (e) selenim film doped by iodine at $T = 363$ K for 6 h with a heating speed of 1 K min^{-1}.

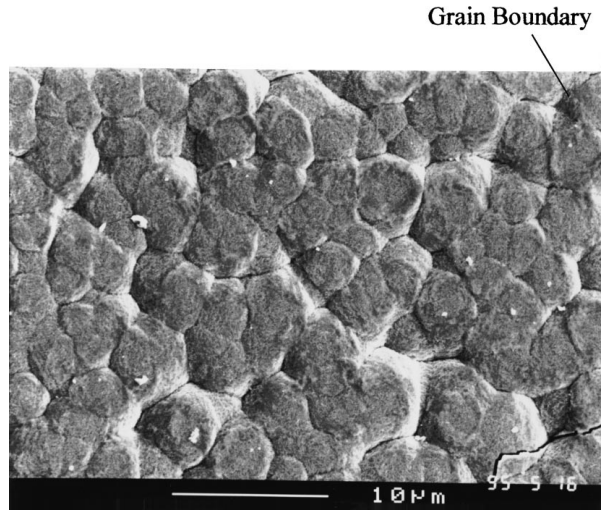

Figure 3 Microphotography of a pure selenium film crystallyzed at 363 K for 6 h.

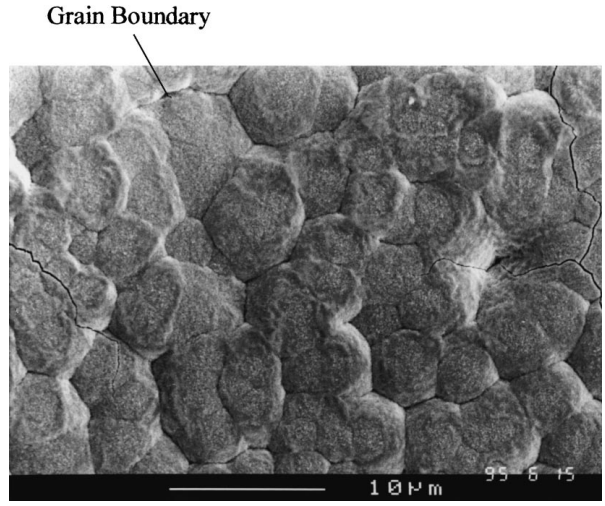

Figure 4 Microphotography of a selenium film crystallyzed at 363 K for 6 h and post annealed under iodine atmosphere 1 h at 363 K.

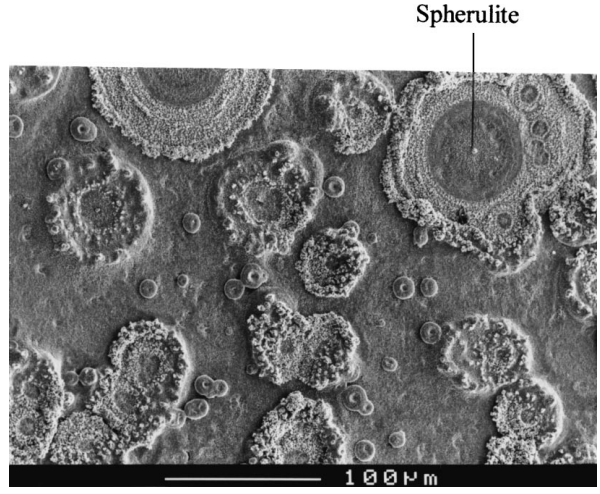

Figure 5 Microphotography of a selenium film iodine post doped in room conditions.

the spherulites which induces depleted domains with a high density of pinholes between the spherulites domains (Fig. 6) the depleted domains are made of small crystallites. The spherulites are composed of a

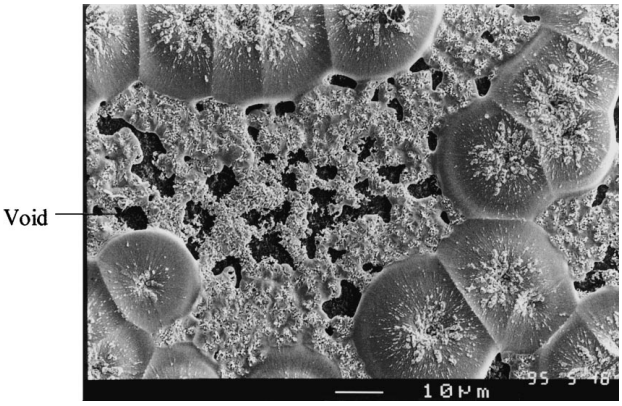

Figure 6 Microphotography of a selenium film iodine post doped at $T = 363$ K for 6 h.

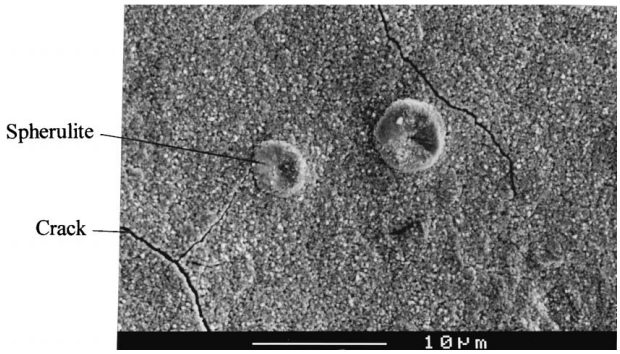

Figure 7 Microphotography of a selenium film iodine post doped at $T = 363$ K for 6 h with a heating speed of 1 K min^{-1}.

smooth circular matrix composed of small crystallites and larger crystallites geometrically shaped radically distributed. It should be noticed that there is about 1 at. % of iodine in the centre of the spherulites where the density of the larger crystallites is higher, while there is 2 to 3 at. % of iodine in the smooth matrix of the spherulites.

When the annealing process controlled i.e. when the temperature is increased at a constant rate of 1 K min^{-1} to achieve the heating temperature (363 K) of the sample, its homogeneity is far higher (Fig. 7). If some cracks are still present, they are not anymore pinholes in the films. Moreover the density of spherulites is far smaller than before and they are at least ten times smaller. The matrix is composed of small crystallites. The spherulites are too small to proceed to iodine composition analysis as above, it should be only say that the average percentage of iodine in the films is about 1 to 2 at. %.

3.3. X.P.S. measurements

Before any ion sputtering a complete XPS spectrum was recorded in order to determine the contamination, if present, of the films. In addition to Se and I peaks only carbon and oxygen peaks are detected. They correspond to classical surface contamination of any sample after room air exposure. The binding energy of the C 1s peak (285 eV) will be used as a reference [17].

For depth profiling all XPS spectra were recorded under identical conditions. The depth profiling is reported in Fig. 8. There is a higher amount of iodine at the surface of the films (1.5 at. %). In the bulk the atomic percentage of iodine stabilised at about 0.3 at. %.

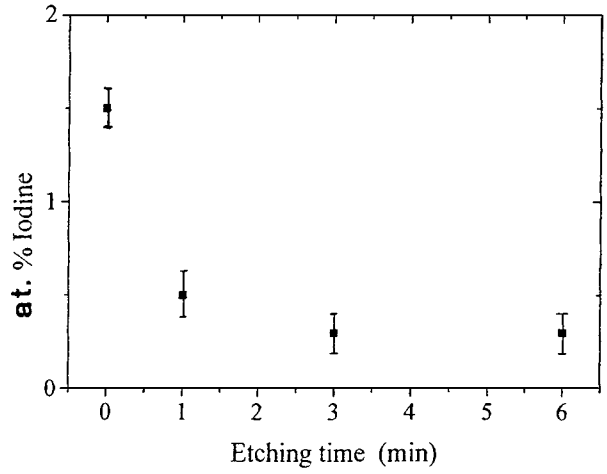

Figure 8 XPS depth profilling of the iodine.

Nearly similar results are obtained for each sample obtained by iodine doping of initially amorphous films.

In the case of doping of crystallised layers, within the accuracy of the method, no iodine has been detected.

It should be noted that the oxygen contamination peak disappears after three minutes of etching.

3.4. Raman scattering study

A typical Raman spectrum of films doped with iodine during crystallisation is reported in Fig. 9. Two intense peaks centred at 144 and 236 cm^{-1} are observed (Fig. 9). When the scale is magnified (insert Fig. 9) new peaks and peak shoulders appear.

The two main peaks of the Raman spectra can be assigned to the very intense first order peaks of the trigonal selenium, which is the result expected, the selenium being the main component of the films. Carrol and Lannin [18] have reported that these two peaks are centred at 143 and 235 cm^{-1} while Lucovsky and col [19] have earlier estimated these peaks at 144 and 225 cm^{-1}.

Is has been shown that these first order peaks are 100 times more intense than the second order peaks in selenium [18]. Therefore some of the peaks visualised in the magnified spectrum can correspond to selenium second

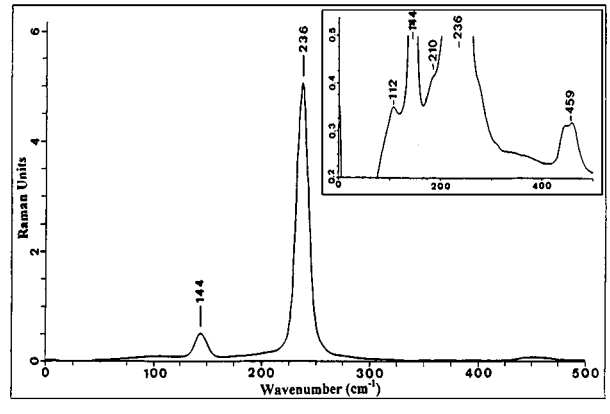

Figure 9 Raman spectra Insert: magnifying of the spectrum.

order peaks. The envelope of the high frequency band and its frequency (459 cm^{-1}) allows to assign this band to the high frequency optic band of hexagonal selenium [18], the features which have not been attributed correspond to iodine. Extensive Raman studies of iodine compounds have been performed [20–22]. These studies yielded a fundamental at 180 cm^{-1} for aggregated iodine labelled (I_2) n while isolated I_2 fundamental was observed at 212 cm^{-1}. Maki and Rorneris [20] have shown that the triodide ion I_3^- shows bands $\nu 1$ and $\nu 3$ at 112 cm^{-1} and 145 cm^{-1}. Therefore the small peak in the spectrum of Fig. 9 can be attributed to the $\nu 1$ band of I_3^-; the $\nu 3$ band cannot be discriminated from the more intense selenium band. The shoulder situated around 210 cm^{-1} corresponds to I_2.

We have shown by Raman scattering study that the selenium films contain iodine, mainly in the I_3^- state but also some isolated I_2.

3.5. Influence of the doping process on the conductivity

Ohmic contacts are not easy to obtain with selenium, El Azab and Champness [23] have shown that ohmic contacts were obtained with Te, but they have worked with monocrystalline selenium films on Te single crystal, which is not the case in the present work. With Te polycrystalline films, ohmic contacts are not so easy to obtain. Gold contacts are more suitable, however when the voltage increases there was some discrepancy with ohmicity, therefore we have used chromium contacts which gives the best results in the present case (Fig. 1). The room temperature conductivities of the samples are reported Table I, and the variation of the conductivity with the reciprocal temperature is reported Fig. 10.

Before iodine treatment the room temperature conductivity of the crystallised films is around $10^{-8}\ \Omega^{-1}\ cm^{-1}$ (Fig. 10a). It can be seen Fig. 10b that, after iodine treatment the room temperature conductivity is one order of magnitude higher. However at a temperature $T = 400$ K the conductivity decreases steeply by one order of magnitude. Then, when the temperature is decreased to the room temperature, the conductivity is nearly the same than before annealing under iodine atmosphere (Fig. 10c). However if we proceed to conductivity measurements below 370 K there is no evolution of the conductivity from one measurement to another one.

TABLE I Room temperature conductivity and activation energy

Selenium film	σ $(\Omega^{-1}\ cm^{-1})$	ΔE (eV)
Pure polycrystalline annealing ($T = 363$ K, 6 h)	1.1×10^{-7}	
Obtained from predoped powder [16]	1.5×10^{-5}	0.3–0.6
Doped with iodine 1 h at 363 K after crytallization	8×10^{-7}	0.30
The same sample after annealing at $T > 400$ K	1.5×10^{-7}	0.31
Crystallized under iodine atmosphere at 363 K for 6 h. Heating rate: 1 K min^{-1}	5×10^{-4}–5×10^{-3}	0.33
Single crystal	10^{-4}–10^{-5}	

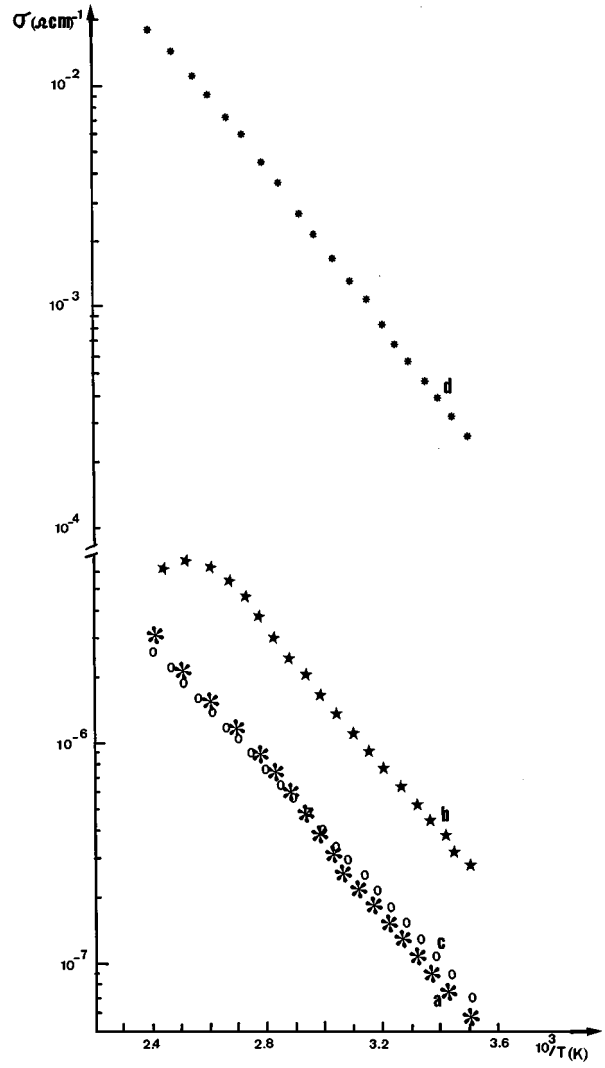

Figure 10 Conductivity variation with the reciprocal temperature, (a) polycrystalline selenium film, (b) polycrystalline selenium film post doped with iodine, (c) polycrystalline selenium film post doped with iodine after annealing at $T > 400$ K, (d) polycrystalline selenium film crystallized under iodine atmosphere.

In the case of selenium films crystallised under iodine atmosphere, the room temperature conductivity is five order of magnitude higher than that of pure selenium films. Even if at high temperature (>400 K) there is some decrease of the conductivity (Fig. 10d) it stays far higher than that of pure Se films.

4. Discussion

All the results described above have shown that the properties of the iodine doped polycrystalline films are very sensitive to the iodine doping process.

When the samples are iodine doped after the crystallisation the iodine effect is quite small. The texture of the polycrystalline selenium films is not modified and the conductivity increases slightly, moreover in those samples no iodine have been detected which does not means that there is not any iodine in the films but that the sensitivity of the techniques used (microprobe analysis, XPS) is not sufficient to detect the very small quantity of iodine present in the films. This behaviour is quite similar to that of polycrystalline transition metal dichalcogenides (MX_2) post annealed 1 h at 373 K in

iodine atmosphere [24]. After this treatment the electrical conductivity of these films is improved (multiplied by 5 to 25). It has been shown earlier that the conductivity of polycrystalline selenium films is controlled by grain boundary scattering mechanisms. It is well known that grain boundaries in polycrystalline films are disordered regions with a very high density of dangling bonds. In the case of selenium films obtained from iodine doped powder we have shown that iodine mainly segregates at the grain boundary [7]. Therefore, since there is no modification of the structure of the films, it is probable that the small increase of the conductivity after annealing under iodine atmosphere of polycrystalline films should be attributed to iodine diffusion at the grain boundaries. It has been shown in the case of MX_2 films that there is iodine passivation of dangling bonds at the grain boundaries, which decreases their scattering effect and allows the improvement of the conductivity. It appears that the same iodine influence occurs in these selenium polycrystalline films.

When the temperature used during the conductivity measurements is higher than 400 K the conductivity decreases towards its value before iodine treatment, while if we proceed to conductivity measurements below 370 K there is no evolution of the conductivity from one measurement to another one. Therefore we can imagine that there is some iodine loss at high temperature ($T > 395$ K). Probably the iodine escapes from the grain boundaries, which explains that the film conductivity goes back to its value before doping.

It appears that different results are obtained when doping takes place during crystallisation of the films. The iodine influence on the properties of the polycrystalline films is highest and depends strongly on the annealing conditions. Here the polycrystalline spherulites are initiated by iodine at room temperature, which demonstrates the great influence of iodine on selenium crystallisation. The ageing of amorphous selenium films at room temperature have been systematically studied by Audiere and col [25], they have shown that the selenium films crystallise slowly with some spherulites formation. They have shown that the crystallisation increases when the films are in a water-saturated atmosphere. Chiang and Johnson [26] have shown that the same effect occurs in others chemical vapours such as carbon disulphide, isopropyl acetate and trichloroethylene. They have shown that the time required to notice any visual sign of crystallisation on the Se surface for water vapour was of the order of several weeks, whereas for CS2, trichloroethylene and isopropylacetate it was one day, three days and six days respectively, in the case of our works, the time required was less than 24 h in iodine atmosphere.

They have attributed this fast surface crystallisation to the high surface mobility of Se molecules in the presence of the chemical vapours which induces agglomeration of crystallites of Se in some selective "center area" such as foreign particle or surface irregularity.

In the case of halogens it has been shown that, if small amounts of iodine (up to 55 ppm) inhibits the crystallisation of selenium, however, for higher concentration ($>$1000 ppm) the crystallisation time decreases when the iodine doping concentration increases [27]. In the present work high doping concentration have been used. It is well known that halogen (Cl, Br and I) are often used as transport agent to obtain single crystals of chalcogen compounds [28, 29], therefore in the present work, the iodine vapour facilitates the surface migration of selenium atoms by increasing their mobility. The moving selenium atoms accumulate at the surface defaults of the layers, which induces formation of crystallites with spherulite shapes. This initialisation of the crystallisation increases strongly the crystallisation speed of the amorphous films at room temperature.

When the temperature is increased in the presence of iodine the effect is amplified. Audiere and col (25 b) have shown that the spherulite density increases when the annealing temperature is increased. Therefore at 363 K there is a lot of spherulites while the large mobility of selenium atoms induced by iodine atmosphere implies pinhole formation. The heating rate is quite fast ($\geq$5 K min^{-1}) therefore, the dilatation coefficient of a-Se and of the substrate being different, some constraint domains will appear during heating which will induce active area for crystallisation. To prevent these effects it is necessary to control more accurately the annealing process. When the samples are kept at the room temperature large spherulites appear at the main surface defaults, when the samples are quickly heated (heating rate $\geq$5 K/min) all the defaults and induced constraints initiate spherulites and their density is large. When the heating rate is constant and small (1 K/min) there is not large constraints in the film and even if, as systematically in selenium [30], some spherulites appear, the iodine interacts with selenium all over the surface and not only with the defaults of the surface. Therefore nucleus density is very high which induces a high density of small crystallites, which then agglomerate to form large grains while the growth of the spherulites is limited by this crystallisation. It has been shown by XPS that there is iodine all over the thickness of the films: progressively the iodine diffuses though the layer and the selenium films crystallise all over the thickness.

It has been shown that there are two types of crystallisation induced either in the bulk (bulk-induced crystallisation: BIC) or at the surface (surface-induced crystallisation: SIC) [31, 32]. In the present work, since the crystallisation process is modified by the presence of gaseous iodine it appears that SIC is the dominating process, at least at the beginning of the crystallisation.

The iodine concentration obtained by microprobe analysis is not very different from that obtained by XPS at the surface of the film. After etching the iodine concentration obtained by XPS is smaller that the average value obtained by microprobe. This discrepancy could be attributed to the etching effect; probably the iodine-sputtering yield is higher than that of selenium.

In the case of the films crystallised under iodine atmosphere, the small decrease of the conductivity, at high temperature should be attributed, here also, to some iodine escape from the grain boundaries. However it stays far higher than that of pure Se. Therefore, if the iodine release from the grain boundaries can explain the decrease of the conductivity of the doped films after

heating at high temperature ($T < 400$ K), iodine doping cannot explain classically, as in the case of usual semiconductors the strong increase of the conductivity.

It has been shown earlier that iodine modifies the conductivity of the films by altering the conditions on the grain boundaries, but that the hole concentration is not changed [33, 34]. It can be seen Table I that the activation energy of the iodine doped samples is about 0.3 eV, and that it is not dependent of the absolute value of the conductivity. This stability shows that there is no shift of the Fermi level in the crystallites, which excludes true doping effect of the crystallites. Therefore the present increase of the conductivity of the films crystallized under iodine athmosphere should be related to the higher crystalline quality of the of these films (Fig. 2). Even if there is some iodine escape from the grain boudaries at $T > 400$ K, the selenium crystallites stay larger, which decreases the grain boundary effect and allows an improvement of the conductivity.

5. Conclusion

It has been shown that iodine post doping of polycrystalline selenium films does not modify the structural properties of the films, while the conductivity increases by a factor of 8. This small improvement is attributed to dangling bond passivation by iodine at the grain boundaries. More significative is the effect of iodine when it is present during the crystallisation process. At room temperature iodine addition increases the mobility of the selenium atoms at the surface of the films, which induces spherulites formation, the process being accelerated when the temperature is quickly increased. When the heating rate is controlled ($1\ \mathrm{k} \cdot \mathrm{min}^{-1}$) the crystallisation process is more homogeneous, the structural quality and the conductivity of the films are far higher. The high conductivity could be attributed to the crystalline quality of the layer.

Acknowledgements

The authors wish to thank. Mr P. Le Ray for performing Raman measurements and Mr L. Assmann for X.R.D. measurements and Mrs Barreau A. and Le Ny R. for SEM and microprobe studies.

References

1. K. S. KIM and D. TURNBULL, *J. Appl. Phys.* **44** (1973) 5237.
2. *Idem., ibid.* **45** (1974) 3447.
3. G. GROSS, R. B. STEPHENS and D. TURNBULL, *ibid.* **48** (1977) 1139.
4. J. P. AUDIERE, CH. MAZIERES and J. C. CARBALLES, *Journal of Non-Crystalline Solids* **34** (1979) 37.
5. E. A. CHATTERJEE and S. P. SEN GUPTA, *Journal of Materials Science Letters* **5** (1986) 559.
6. N. G. PATEL, B. H. LASHKARI, C. J. PANCHAL and K. K. MAKHIJA, *Cryst. Res. Technol.* **29** (1994) 859.
7. G. SAFOULA, J. C. BERNEDE, A. LATEF, E. RZEPKA and M. SPIESSER, *Mater. Chem. and Phys.* **20** (1988) 571.
8. J. C. BERNEDE, G. SAFOULA, R. MESSOUSSI, A. BONNET and A. CONAN, *J. Phys. Chem. Solids* **50** (1989) 1159.
9. R. MESSOUSSI, J. C. BERNEDE, G. SAFOULA, E. RZEPKA and M. SPIESSER, *Physica. Stat. Sol. (a)* **123** (1991) 175.
10. J. ROWLANDS and S. KASAP, *Physics Today*, November 1997, 24.
11. J. W. BOAG, *Xeroradiography, Phys. Med. Bio1* **18** (1973) 3.
12. R. A. ZINGARO and W. C. COOPER, Selenium (Van Nostrand/Reinhald Co., New-York, 1974).
13. C. H. CHAMPNESS, *J. Appl. Phys.* **32** (1987) 919.
14. H. P. D. LANYON, *Phys. Stat. Sol. (a)* **2** (1970) 287.
15. S. POGANSKI, *Zeitschnift Für Physik* **134** (1953) 469.
16. E. F. KAELBLE, "Handbook of X-Rays," (McGraw-Hill, New-York, 1967).
17. DR. BRIGGS and M. P. SEAH, Pratical Surface Analysis Vol. 1-Auger and X-Rays Photoelectron Spectroscopy (John Wiley & sons, 1990) p. 543.
18. P. S. CARROLL and J. S. LANNIN, *Phys. Rev. B* **27** (1983) 1028.
19. G. LUCOVSKY, R. C. KEEZER and E. BURSTEIN, *Solid State Communications* **5** (1967) 439.
20. A. G. MAKI and R. RORNERIS, *Spectrochimica Acta* **23A** (1967) 867.
21. W. F. HOWARD and L. ANDREWS, *Journal of Raman Spectroscopy* **2** (1974) 447.
22. L. ANDREWS, E. S. PROCHASKA and A. LOEWENSCHUSS, *Inorg. Chem.* **19** (1980) 463.
23. M. I. EL-AZAB and C. H. CHAMPNESS, *IEEE Trans. Elect. Dev.* **ED-27** (1980) 255.
24. J. C. BERNEDE, H. HADOUDA, S. J. LI, H. ESSAIDI, J. POUZET and A. KHELIL, *J. Phys. III* **6** (1996) 1697.
25. J. P. AUDIERE, C. MAZIERES and J. C. CARBALLES, *Journal of Non-Cystalline Solids* **27** (1978) 411 (a) and **34** (1979) 37 (b).
26. Y. S. CHIANG and J. K. JOHNSON, *J. Appl. Phys.* **38** (1967) 1647.
27. M. B. IJANJUA, J. M. TOGURI and W. C. COOPER, *J. Can. Phys.* **49** (1970) 475.
28. M. K. AGARWUAL and V. V. RAO, *Cryst. Res. Technol.* **24** (1989) 1215.
29. C. H. CHAMPNESS and R. H. HOFFMAN, *Journ. Non-Crystalline Solids* **4** (1970) 138.
30. J. BAGLIO, *J. Sol. Sat. Chem.* **49** (1983) 166.
31. K. ZELLAMA, P. GERMAIN, S. SQUELARD and J. C. BOURGOIN, *J. Appl. Phys.* **50** (1979) 6995.
32. G. FLEURY, C. LHERMITTTE and G. VIGER, *Journ. Non-Crystalline Solids* **46** (1981) 427.
33. J. HELESKIVI, T. STUBB and T. SUNTOLA, *J. Appl. Phys.* **40** (1969) 2923.
34. K. W. PLESNER, *Proc. Phys. Soc.* **B64** (1951) 671.

Received 2 June
and accepted 14 December 1999